Hot carrier relaxation and inhibited thermalization in superlattice heterostructures: The potential for phonon management © ©

Cite as: Appl. Phys. Lett. **118**, 213902 (2021); https://doi.org/10.1063/5.0052600 Submitted: 31 March 2021 • Accepted: 06 May 2021 • Published Online: 26 May 2021

🗓 Hamidreza Esmaielpour, 🗓 Brandon K. Durant, 🗓 Kyle R. Dorman, et al.

COLLECTIONS

Paper published as part of the special topic on Scalable Ways to Break the Efficiency Limit of Single-Junction Solar Cells

- F This paper was selected as Featured
- SCI This paper was selected as Scilight







ARTICLES YOU MAY BE INTERESTED IN

Challenges, myths, and opportunities in hot carrier solar cells

Journal of Applied Physics 128, 220903 (2020); https://doi.org/10.1063/5.0028981

Identification of surface and volume hot-carrier thermalization mechanisms in ultrathin GaAs layers

Journal of Applied Physics 128, 193102 (2020); https://doi.org/10.1063/5.0027687

Enhanced light-matter interactions at photonic magic-angle topological transitions Applied Physics Letters 118, 211101 (2021); https://doi.org/10.1063/5.0052580

☐ QBLOX



Shorten Setup Time
Auto-Calibration
More Qubits

Fully-integrated
Quantum Control Stacks
Ultrastable DC to 18.5 GHz
Synchronized <<1 ns
Ultralow noise



visit our website >



Hot carrier relaxation and inhibited thermalization in superlattice heterostructures: The potential for phonon management () (3)

Cite as: Appl. Phys. Lett. **118**, 213902 (2021); doi: 10.1063/5.0052600 Submitted: 31 March 2021 · Accepted: 6 May 2021 · Published Online: 26 May 2021







Hamidreza Esmaielpour, De Brandon K. Durant, De Kyle R. Dorman, De Vincent R. Whiteside, De Jivtesh Garg, De Tetsuya D. Mishima, Michael B. Santos, De Ian R. Sellers, De Jean-François Guillemoles, De Jivtesh Garg, De

AFFILIATIONS

- ¹CNRS-Institute Photovoltaïque d'Ile de France (IPVF), UMR IPVF 9006, 91120 Palaiseau, France
- ²Department of Physics and Astronomy, University of Oklahoma, Norman, Oklahoma 73019, USA
- School of Aerospace and Mechanical Engineering, University of Oklahoma, Norman, Oklahoma 73019, USA

Note: This paper is part of the APL Special Collection on Scalable Ways to Break the Efficiency Limit of Single-Junction Solar Cells.

a) Authors to whom correspondence should be addressed: sellers@ou.edu and daniel.suchet@polytechnique.org

ABSTRACT

One of the main loss mechanisms in photovoltaic solar cells is the thermalization of photogenerated hot carriers via phonon-mediated relaxation. By inhibiting these relaxation mechanisms and reducing thermalization losses, it may be possible to improve the power conversion efficiency of solar cells beyond the single gap limit. Here, type-II InAs/AlAsSb multi-quantum well (MQW) structures are investigated to study the impact of the phononic properties of the AlAsSb barrier material in hot carrier thermalization. Experimental and theoretical results show that by increasing the barrier thickness (increasing the relative contribution of AlAsSb content in the superlattices), the relaxation of hot carriers is reduced as observed in power-dependent photoluminescence and thermalization analysis. This is attributed to an increase in the phononic bandgap of the MQW with increasing AlAsSb composition reducing the efficiency of the dominant Klemens mechanism as the phononic properties shift toward a more AlSb-like behavior.

Published under an exclusive license by AIP Publishing. https://doi.org/10.1063/5.0052600

Designing hot carrier absorbers with long hot carrier lifetimes would have significant impact on the realization of hot carrier solar cell technology. By studying the origin of hot carrier dynamics and tailoring the properties of materials to inhibit hot carrier relaxation, there is a potential to develop technology in which hot photogenerated carriers contribute to the operation of a new generation of optoelectronic devices. In polar semiconductors, the relaxation of hot carriers typically occurs through interactions with longitudinal optical (LO) phonons via Fröhlich coupling.² Specifically, shortly after photoabsorption, high energy photogenerated "hot" carriers lose their excess kinetic energy by emitting LO-phonons, which is then followed by the decay of these high energy optical phonons into lower energy acoustic phonons through Klemens³ and Ridley⁴ processes. The formation of a long-lasting hot carrier population thus requires methods to inhibit phonon relaxation pathways that facilitate hot carrier relaxation, therefore extending the lifetime of the non-equilibrium carrier population.

The reduction (or even suppression) of phonon-mediated hot carrier thermalization may be addressed either by inhibiting Fröhlich interactions or through approaches to enhance the re-absorption of hot LO-phonons back into the carrier distribution prior to heat dissipation. This second approach requires a "phonon bottleneck," i.e., a reduction of the optical phonon decay rate, such that a hot phonon population can form.

Several approaches have been investigated to engineer such a phonon bottleneck. Quantum well (QW) structures have shown the potential to increase hot carrier lifetimes longer than that in bulk semiconductors. The origin of this effect is attributed to the suppression of phonon-mediated relaxation channels and the creation of a non-equilibrium phonon population (hot phonons) in the system, which then stabilizes a hot carrier distribution. Another technique to create the phonon bottleneck effect is to control the Klemens and Ridley mechanisms via manipulating the material properties. It has been

⁴CNRS-Ecole Polytechnique, UMR IPVF 9006, 91120 Palaiseau, France

shown that utilizing semiconductors with large phononic band gaps, like AlSb and InN, can inhibit the decay of high energy optical phonons due to the suppression of the Klemens mechanism. ¹⁰ In addition, it may also be possible to tailor the phononic properties of materials using QW structures. ⁹

While hot carrier effects have already been observed in various low dimensional systems, 11–14 type-II InAs multi-quantum wells (MQW) have shown potentially interesting effects for practical hot carrier solar cell applications, such as relatively low hot carrier threshold, 15,16 evidence of intervalley scattering, 17,18 and the suppression of the Klemens mechanism due to the presence of large phononic band gaps. In this work, type-II InAs/AlAsSb MQW structures with increasing AlAsSb (barrier) contributions are investigated to assess the potential of controlling carrier thermalization via quantum confinement and phononic engineering. This system, in addition to significant carrier confinement in the conduction band, also provides a considerable mismatch in the phononic properties, therefore providing the potential for decoupling of relaxation pathways by design.

The type-II InAs/AlAs_{0.16}Sb_{0.84} MQW structures (p-i-n diodes) investigated here were grown by molecular beam epitaxy on p+-GaAs substrates. Prior to the deposition of the active region, the substrate was heated to 580 °C to remove any residual oxide. Before the growth of the multi-quantum well structures, a 1 µm thick AlAs_{0.16}Sb_{0.84} buffer layer was deposited to enable relaxation of strain and defects at the lower GaAs/AlAsSb interface, therefore improving the quality of the nominally lattice matched InAs QWs grown above. The active region of these three structures consisted of ten 2.1 nm QWs isolated by symmetric AlAs_{0.16}Sb_{0.84} barriers of thickness 2.1, 5.2, or 10 nm for the three MQW structures studied. The active region was completed with a 30 nm AlAs_{0.16}Sb_{0.84} barrier followed by a thin 5 nm GaSb capping layer to prevent oxidation of the high Al-containing barrier materials. The schematic of the sample and the band energy diagram of the active region are shown in Fig. 1(a). Full details of the growth parameters are described elsewhere. 16

Photoluminescence (PL) measurements were recorded using a hyperspectral imaging technique, which creates a spectrally (with 2 nm resolution) and spatially resolved (down to the micrometer scale) PL maps across the sample. The absolute photon flux emitted by the MQWs is determined via applying various calibration techniques (spatially, spectrally, and intensity calibrations). The hot carrier properties of the samples are studied at various lattice temperatures and excitation powers under continuous wave laser excitation (532 nm). Figure 1(b) shows the absolute photon flux emitted by the 5.2 nm AlAsSb barrier sample at various excitation powers at 300 K. With increasing excitation power, the high energy tail of the emission spectrum broadens, which is indicative of the presence of hot carriers in the steady state system. The optical and thermodynamic properties of the emitting particles in the semiconductor are determined by fitting the PL spectrum with a generalized Planck's law as follows: 1,2,11

$$I_{PL}(E) = \frac{2\pi A(E)E^2}{h^3c^2} \exp\left[\left(\frac{E - \Delta\mu}{k_BT}\right) - 1\right]^{-1},$$
 (1)

where A(E) is the absorptivity of the sample, "c" is the speed of light, "h" is the Planck constant, k_B is the Boltzmann constant, $\Delta\mu$ the quasi-Fermi level splitting (assumed to be constant across all wells), and I_{PL} the emitted PL intensity.

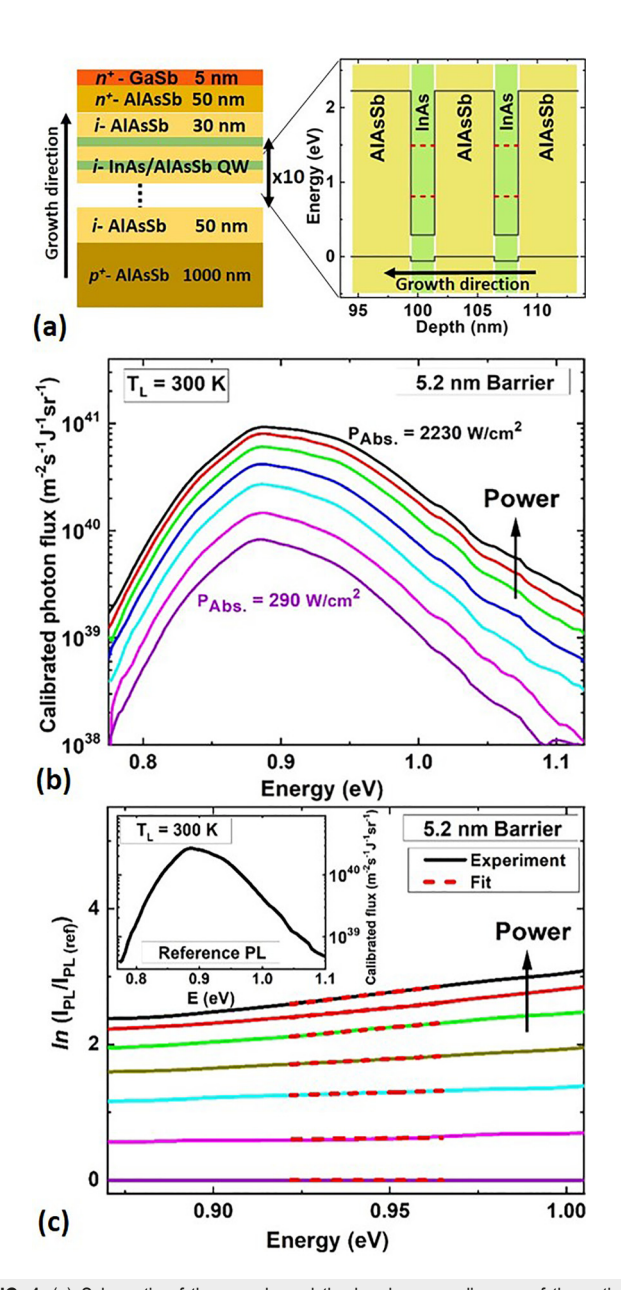


FIG. 1. (a) Schematic of the sample and the band energy diagram of the active region. The red dashed lines indicate the position of the discrete energy levels within the QW. Three MQWs with barrier thicknesses 2.1, 5.2, and 10 nm are grown. (b) PL spectra at 300 K emitted by the InAs MQW with 5.2 nm barrier at various excitation powers. (c) Spectral PL ratios of the MQW structure at 300 K. The dashed red lines indicate the ranges of energy, where the carrier temperatures are determined. The inset shows the reference PL spectrum emitted at the lowest excitation power.

While this method has been used extensively in the hot carrier community, ^{2,11,12,14,15,22} it represents a simple analytic method to deduce the qualitative temperature of the carriers in the system. It is only strictly valid in bulk materials in which the exponential pre-factor is approximately constant above the bandgap, and where effects such

as state filling and redistribution of carriers into non-degenerate bands in the continuum are not significant. Otherwise, a more comprehensive consideration of the absorptivity must be included such as in recent work of Gibelli *et al.*²³ and for the specific system considered here, by Whiteside *et al.*²⁴

To eliminate the complexities of such analysis, here a PL ratio method is applied to determine the temperature of hot carriers in the system.²⁵ This method simplifies the analysis of hot carrier effects in the PL such that the contribution and complexity of the absorptivity at high excitation powers can be avoided by using a low power reference, see Fig. 1(c), where the spectrum is considered at equilibrium with the lattice, or that those carriers in the Γ -valley are fully thermalized. This reference is used to produce spectral ratios that are proportional to the carrier temperature while removing any energy dependence of the absorptivity related to effects, such as state filling or redistribution of carriers in the system; this would cause the emissivity term in Eq. (1) to become energy dependent, limiting or even invalidating hot carrier analysis using this method.²⁵ This important consideration is often not well considered in the literature, particularly in emerging materials where the inhomogeneously broadened contribution of multiple transitions inhibits any real quantitative analysis of hot carriers from the PL spectrum. The dashed red lines in Fig. 1(c) indicate the range of energies used to extract the carrier temperatures.

Figure 2(a) shows the extracted temperature difference (ΔT : the temperature difference between non-equilibrium carriers and the lattice) vs thermalized power (P_{th}) for the three MQW structures at 300 K using the ratio method described above. To assess the performance of the MQWs in suppressing phonon mediated thermalization of hot carriers, it is required to determine the fraction of the absorbed power density above the band edge of the semiconductor, namely the thermalized power (P_{th}). The thermalized power is determined by 26

$$P_{th} \approx \frac{E_{laser} - E_{gap}}{E_{laser}} P_{abs},$$
 (2)

where "E_{laser}" and "E_{gap}" are the laser and the bandgap energies, respectively, and "P_{abs}" is the absorbed power density within the active region determined by transfer matrix methodology.^{27,28} Photo-absorption in each device is determined by considering the total thickness of the potential wells and the barrier materials. The refractive indices of bulk materials are applied for the analysis. Figure 2(a) indicates that upon increasing the excitation power, the photo-generated carriers become "hotter," which is consistent with the presence of an LO phonon bottleneck as observed in several other quantum well systems.^{27,11}

Moreover, the MQW structure with the largest barrier thickness (10 nm) shows the largest ΔT at a given absorbed power density as indicated on the upper x-axis in Fig. 2(a). This larger ΔT is indicative of stronger hot carrier effects in the 10 nm sample. Furthermore, the presence of a phonon bottleneck is also apparently dependent upon the barrier thickness, with the 10 nm sample displaying hot carrier effects at lower excitation densities, followed by the 5.2 nm, and 2.1 nm barrier structures, respectively. This not only suggests that the AlAsSb barriers have a strong role in inhibiting carrier thermalization in these structures, but that the activation or control of a phonon bottleneck can be initiated via the incorporation of AlAsSb in the system, by design.

Interestingly, the threshold for hot carrier generation and total excess (hot carrier) temperature induced (ΔT) are somewhat lower than those typically observed in other III–V systems investigated in

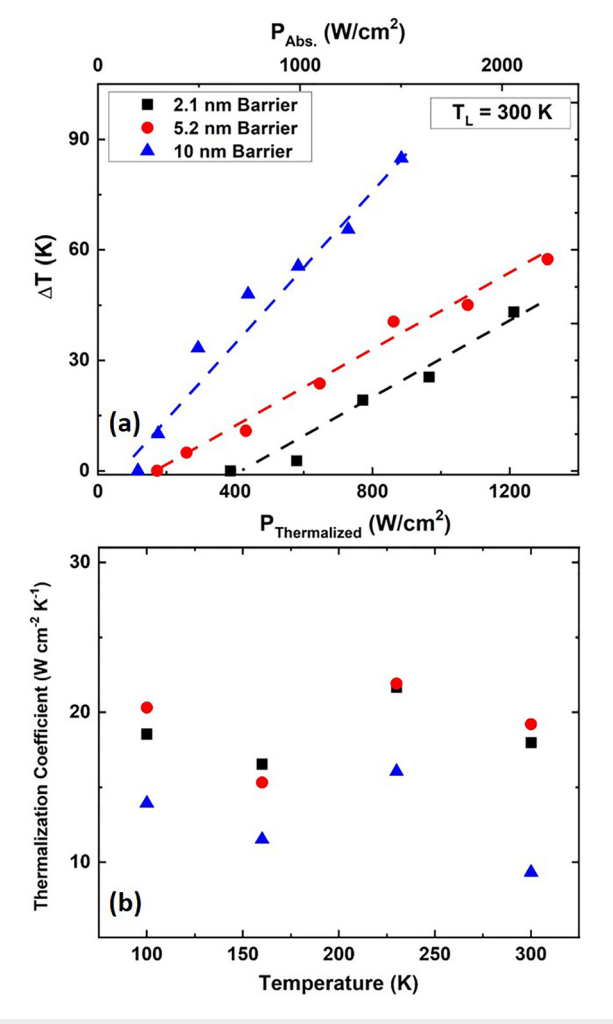


FIG. 2. (a) ΔT as a function of the thermalized and the absorbed power at 300 K for the MQW structures with 2.1 nm (black), 5.2 nm (red), and 10 nm (blue). The dashed lines indicate the results of the linear fit, which are inversely proportional with the thermalization coefficient of each sample. (b) Thermalization coefficient as a function of the lattice temperature for the MQW structures.

the literature. $^{11-13}$ In the case of the lower threshold, these lower excitation levels have been observed previously 15,16 and the presence of a bottleneck occurs at excited carrier densities of $\sim\!10^{12}\,\text{cm}^{-2}$ [5000 suns, see Fig. 2(a)], orders of magnitude lower than typically seen in type-I quantum wells. 11 While the total excess energy (ΔT) provided (up to $\sim\!90\,\text{K}$) is less than that observed elsewhere at larger excitation fluencies, this may be associated with intervalley scattering that is prevalent under high energy photoexcitation in these systems. 17,18,29

Figure 2(a) indicates a linear dependence between the thermalized power and ΔT . Such behavior is well described by the thermalization of high energy hot photo-generated carriers by the emission of LO phonons via Fröhlich interactions.^{7,11,30} Therefore, the dissipation of excess energy via the emission of heat can also be qualitatively described by the thermalization coefficient of hot carriers (Q) in MQW structures by applying a linear fit to the results in Fig. 2. The

slopes are inversely proportional to the thermalization coefficient, as described by 14,26

$$P_{th} = Q \cdot \Delta T. \tag{3}$$

The thermalization coefficient of hot carriers for the MQW structures under investigation at various lattice temperatures is plotted in Fig. 2(b). It is observed that the thermalization coefficient of the individual samples does not change significantly as a function of lattice temperature, which may be a further indication that the relaxation of hot carriers follows a more subtle relaxation pathway involving not only LO phonons and the Klemens process, but also interactions with intervalley phonons and carrier scattering into the higher order satellites. 31 However, despite the unusual temperature independence of the samples under investigation, the MQW structure with the thickest barrier (10 nm) again shows the lowest values as compared to other structures, further supporting the role of the AlAsSb in inhibiting carrier thermalization. A small thermalization coefficient is indicative of smaller hot carrier thermalization losses, which can lead to stronger hot carrier effects in the system. The values of Q extracted here suggest potential power conversion efficiencies in excess of 35%³² for this unoptimized single gap system.

While others have assessed the viability of phonon engineering with different conclusions, 7,9,33 here the origin of the apparent control of carrier thermalization through phonon engineering is attributed to the specific and somewhat unique properties of the InAs/AlAsSb system studied with respect to those in earlier works. First, the phononic mismatch in this system is significant, which when coupled with the type-II nature of the superlattice—whereby electrons (InAs) and holes (AlAsSb) are confined in spatially separated wells—enhances the role of the barriers in the transport, recombination, and dynamics of the system.³⁴ Furthermore, the extent of the electron and more dramatically the hole wavefunctions throughout the whole InAs/AlAsSb structure has been observed previously to play a strong role in the optical properties and thermalization effects in the system. 16,24,34 As such, it is once more suggested that this system, while encompassing reasonably well established III-V systems, provides a strong test bed for hot carrier physics in semiconductor structures and devices, in which much of the required physics to realize practical hot carrier solar cells and optical devices can be probed and elucidated, as well as being transferable to other systems of interest.

To further elucidate the effects of the superlattice structure on the thermalization of hot carriers in the respective structures under investigation, the effects of the InAs/AlSb superlattice (Fig. 3) composition on the scattering phase space of high energy phonons were determined using density functional theory (DFT) calculations. Here, the AlSb compound is considered for the barrier material to simplify the DFT calculations. This is justified due to the low composition of As (16%) in the AlAsSb barrier. It is well known that InAs has a much smaller phonon bandgap (optical to acoustic phonon energy separation relative to AlSb). 19 This leads to higher optical phonon scattering rates in InAs with respect to AlSb, due predominantly to the dominance of Klemens channel in narrow gap InAs. 19 To assess if a decoupling of the Klemens channel in the InAs QW, or a dominance of the AlSb phononic properties, can inhibit the thermalization rates in the InAs/ AlSb-based MQWs and superlattices investigated, the effect of InAs/ AlSb superlattice composition upon the phonon scattering is calculated through first-principles computations. Figure 3(a) shows the

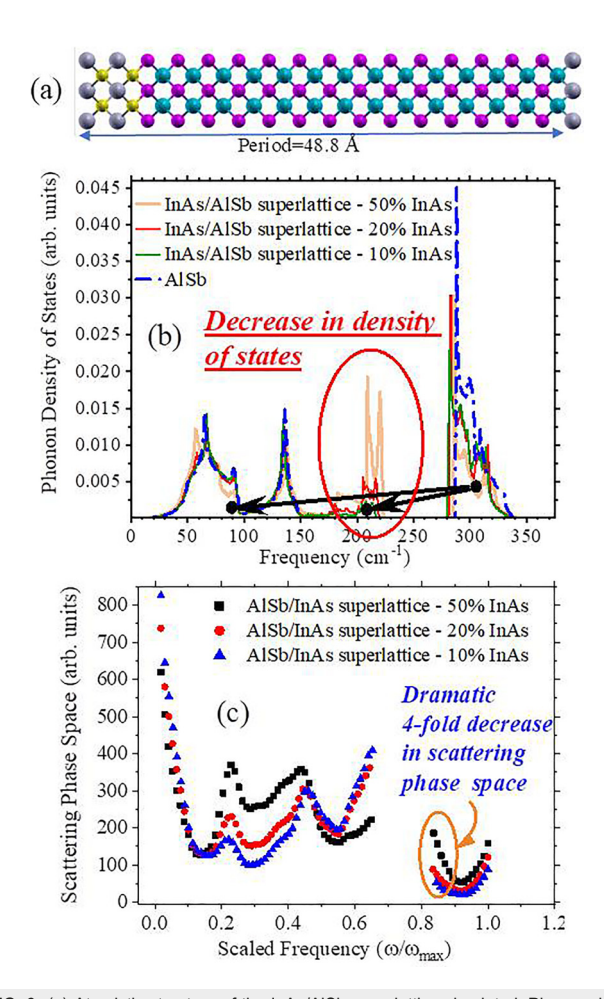


FIG. 3. (a) Atomistic structure of the InAs/AISb superlattice simulated. Phonon density-of-states (b), and scattering phase space (c) for superlattice structures with various InAs compositions (or AISb barrier thicknesses).

atomistic structure of a typical InAs/AlSb superlattice assessed using these techniques.

The approach involves first computing the phonon dispersions of pure InAs, AlSb, and several InAs/AlSb superlattices. As shown in Ref. 19 the density-of-states (DOS) of superlattices cannot be estimated from a simple average of DOS for the two neat compounds, but requires a dedicated calculation.¹⁹ This is achieved by deriving the harmonic interatomic force constants (IFCs) for InAs and AlSb separately from density-functional theory (DFT). IFCs of the superlattice are taken to be an appropriate average of the IFCs for InAs and AlSb (averaged according to a given composition) and combined with the actual atomic mass distribution in the superlattice to compute superlattice phonon dispersion. Since the difference in average masses of InAs and AlSb (\sim 40%) is much larger than the difference in forceconstants (difference in the largest force constants between the two materials is ~10%), the superlattice phonon dispersion is more strongly impacted by mass-difference. As atomic masses are accurately used in this work, the outlined approach leads to accurate superlattice phonon dispersions.

Computed dispersions are used to determine phonon scattering phase space, which is estimated from the number of feasible scattering channels normalized with respect to the wave-vector grid used. DFT calculations are performed in this work using the plane wave pseudo-potential code QUANTUM-ESPRESSO. Norm conserving pseudopotentials in the local density approximation (LDA) were used with a 60 Ry plane wave cutoff. An $8\times8\times8$ Monkhorst mesh was used to describe the electronic properties. For InAs and AlSb, the harmonic force constants were computed on an $8\times8\times8$ q-grid. Acoustic sumrules were imposed to satisfy translational invariance.

The phonon density-of-states for three superlattices (50%, 20%, and 10% InAs, respectively, corresponding to the MQWs with 2.1, 5.2, and 10 nm AlSb barrier thicknesses) and the AlSb compound are shown in Fig. 3(b). It is seen that the InAs/AlSb superlattice with the *largest* InAs composition (50%) has the *smallest phonon bandgap*, yet larger than bulk InAs resulting in phonon scattering between InAs and AlSb.¹⁹ It is evident that by reducing the InAs content (increasing the AlSb contribution) the phonon DOS of the superlattice approaches the behavior of bulk AlSb, with its large phonon bandgap. Such an effect is more evident in the superlattice with 10% InAs composition, where the dramatic decrease in phonon DOS at the frequency range ~220 cm⁻¹ (due to InAs compound) makes the system behave like AlSb, whose maximum frequency for acoustic phonons is ~160 cm⁻¹.

This effect is also consistent with a drop in phonon scattering phase space in frequency ranges between 280 and $340\,\mathrm{cm}^{-1}$ in the superlattices, see Fig. 3(c), due to the suppression of the Klemens mechanism by removing the phonon channels with frequencies of \sim 220 cm⁻¹ (shown by black arrows). The discontinuity in Fig. 3(c) represents the phononic bandgap in the dispersions of these materials. The x-axis of the plot is normalized with respect to ω_{max} which is the maximum phonon frequency for each of the superlattice compositions. A large fourfold decrease in scattering phase is observed at a scaled frequency of \sim 0.85. By decreasing phonon scattering through superlattice composition engineering, it is possible to generate non-equilibrium phonon populations (hot phonons) and create a phonon-bottleneck effect by design, which supports the results in Fig. 2. This suggests that such architectures may be used to establish a hot carrier distribution in a practical quantum well solar cell.

In conclusion, the impact of the barrier thickness of type-II InAs/ AlAs_{0.16}Sb_{0.84} MQW structures in the thermalization of hot carriers is studied. It is seen that by increasing the thickness of the barrier, the prevalence of hot carriers in the system becomes stronger (larger ΔT). This effect is consistent with the low thermalization coefficient of the MQW with the thickest barrier (10 nm, a greater relative AlSb contribution). DFT calculations are carried out to investigate the origin of this effect in superlattice structures by considering various compositions of the constituent compounds. By increasing the contribution of the AlSb barrier (reducing the InAs content in the superlattices), the phononic band structure of the system approaches AlSb-like behavior whose phononic properties can significantly suppress Klemens relaxation pathways. In addition, the DFT calculations indicate that by eliminating the contribution of available InAs phonon states and inhibiting Klemens channels by increasing the thickness of the AlSb barrier, the phonon scattering time increases considerably providing a condition for the creation of hot phonons and, consequently, a strong hot carrier distribution in the MQW structures.

The research is performed within the framework of program 6: PROOF (ANR-IEED-002-02) at IPVF. The authors would like to acknowledge the financial support through the French ANR project ICEMAN (No. ANR-19-CE05-0019). The work performed at the University of Oklahoma has been supported by the United States Department of Energy EPSCoR Program and the Office of Basic Energy Sciences, Materials Science and Energy Division under Award No. DE-SC0019384. J.G. is supported via a National Science Foundation CAREER Award, Grant No. 1847129.

DATA AVAILABILITY

The data that support the findings of this study are available from the corresponding author upon reasonable request.

REFERENCES

- ¹G. Conibeer, N. Ekins-Daukes, J.-F. Guillemoles, D. Kőnig, E.-C. Cho, C.-W. Jiang, S. Shrestha, and M. Green, "Progress on hot carrier cells," Sol. Energy Mater. Sol. Cells **93**, 713–719 (2009).
- ²S. Lyon, "Spectroscopy of hot carriers in semiconductors," J. Lumin. 35, 121–154 (1986).
- ³P. Klemens, "Anharmonic decay of optical phonons," Phys. Rev. **148**, 845 (1966).
- ⁴B. Ridley, "The LO phonon lifetime in GaN," J. Phys.: Condens. Matter **8**, L511 (1996).
- ⁵G. Conibeer, S. Shrestha, S. Huang, R. Patterson, H. Xia, Y. Feng, P. Zhang, N. Gupta, M. Tayebjee, S. Smyth *et al.*, "Hot carrier solar cell absorber prerequisites and candidate material systems," Sol. Energy Mater. Sol. Cells 135, 124–129 (2015).
- ⁶Y. Rosenwaks, M. Hanna, D. Levi, D. Szmyd, R. Ahrenkiel, and A. Nozik, "Hot-carrier cooling in GaAs: Quantum wells versus bulk," Phys. Rev. B 48, 14675 (1993).
- ⁷D. König, Y. Yao, B. Puthen-Veettil, and S. Smith, "Non-equilibrium dynamics, materials and structures for hot carrier solar cells: A detailed review," Semicond. Sci. Technol. 35, 073002 (2020).
- ⁸C.-Y. Tsai, "Theoretical model and simulation of carrier heating with effects of nonequilibrium hot phonons in semiconductor photovoltaic devices," Prog. Photovoltaics 26, 808–824 (2018).
- ⁹H. Levard, "Ingénierie phononique pour les cellules solaires à porteurs chauds," Ph.D. thesis (Université Pierre et Marie Curie-Paris VI, 2015), available at https://tel.archives-ouvertes.fr/tel-01123624.
- ¹⁰Y. Yao and D. König, "Comparison of bulk material candidates for hot carrier absorber," Sol. Energy Mater. Sol. Cells 140, 422–427 (2015).
- ¹¹J. Shah, "Hot carriers in quasi-2-D polar semiconductors," IEEE J. Quantum Electron. 22, 1728–1743 (1986).
- ¹²L. C. Hirst, H. Fujii, Y. Wang, M. Sugiyama, and N. J. Ekins-Daukes, "Hot carriers in quantum wells for photovoltaic efficiency enhancement," IEEE J. Photovoltaics 4, 244–252 (2014).
- ¹³D.-T. Nguyen, L. Lombez, F. Gibelli, S. Boyer-Richard, A. Le Corre, O. Durand, and J.-F. Guillemoles, "Quantitative Experimental Assessment of Hot Carrier Enhanced Solar Cells at Room Temperature," Nat. Energy 3, 236–242 (2018).
- ¹⁴ A. L. Bris, L. Lombez, S. Laribi, G. Boissier, P. Christol, and J.-F. Guillemoles, "Thermalisation rate study of GaSb-based heterostructures by continuous wave photoluminescence and their potential as hot carrier solar cell absorbers," Energy Environ. Sci. 5, 6225–6232 (2012).
- ¹⁵H. Esmaielpour, V. R. Whiteside, J. Tang, S. Vijeyaragunathan, T. D. Mishima, S. Cairns, M. B. Santos, B. Wang, and I. R. Sellers, "Suppression of phonon-mediated hot carrier relaxation in type-II InAs/AlAs_xSb_{1-x} quantum wells: A practical route to hot carrier solar cells," Prog. Photovoltaics 24, 591–599 (2016).
- ¹⁶H. Esmaielpour, V. R. Whiteside, H. P. Piyathilaka, S. Vijeyaragunathan, B. Wang, E. Adcock-Smith, K. P. Roberts, T. D. Mishima, M. B. Santos, A. D. Bristow *et al.*, "Enhanced hot electron lifetimes in quantum wells with inhibited phonon coupling," Sci. Rep. 8, 12473 (2018).

- ¹⁷H. Esmaielpour, K. R. Dorman, D. K. Ferry, T. D. Mishima, M. B. Santos, V. R. Whiteside, and I. R. Sellers, "Exploiting intervalley scattering to harness hot carriers in III–V solar cells," Nat. Energy 5, 336–343 (2020).
- ¹⁸V. Whiteside, H. Esmaielpour, T. Mishima, K. Dorman, M. Santos, D. Ferry, and I. Sellers, "The role of intervalley phonons in hot carrier transfer and extraction in type-II InAs/AlAsSb quantum-well solar cells," Semicond. Sci. Technol. 34, 094001 (2019).
- ¹⁹J. Garg and I. R. Sellers, "Phonon linewidths in InAs/AlSb superlattices derived from first-principles-application towards quantum well hot carrier solar cells," Semicond. Sci. Technol. 35, 044001 (2020).
- ²⁰J. Tang, V. Whiteside, H. Esmaielpour, S. Vijeyaragunathan, T. Mishima, M. Santos, and I. Sellers, "Effects of localization on hot carriers in InAs/AlAs_xSb_{1-x} quantum wells," Appl. Phys. Lett. **106**, 061902 (2015).
- ²¹A. Delamarre, "Développement de nouvelles méthodes de caractérisation optolectroniques des cellules solaires," Ph.D. thesis (Paris 6, 2013), available at https://www.theses.fr/2013PA066501.
- ²²G. Conibeer, Y. Zhang, S. Chung, Y. Liao, S. Bremner, and S. Shrestha, "Multiple quantum wells as slowed hot carrier cooling absorbers in hot carrier cells," IEEE 44th Photovoltaic Specialist Conference (PVSC) (2017), pp. 2186–2191.
- ²³F. Gibelli, L. Lombez, and J.-F. Guillemoles, "Two carrier temperatures non-equilibrium generalized Planck law for semiconductors," Phys. B: Condens. Matter 498, 7–14 (2016).
- ²⁴V. Whiteside, B. Magill, M. P. Lumb, H. Esmaielpour, M. Meeker, R. Mudiyanselage, A. Messager, S. Vijeyaragunathan, T. Mishima, M. Santos et al., "Valence band states in an InAs/AlAsSb multi-quantum well hot carrier absorber," Semicond. Sci. Technol. 34, 025005 (2019).
- ²⁵H. Esmaielpour, L. Lombez, M. Giteau, A. Delamarre, D. Ory, A. Cattoni, S. Collin, J.-F. Guillemoles, and D. Suchet, "Investigation of the spatial

- distribution of hot carriers in quantum-well structures via hyperspectral luminescence imaging," J. Appl. Phys. 128, 165704 (2020).
- 26M. Giteau, E. de Moustier, D. Suchet, H. Esmaielpour, H. Sodabanlu, K. Watanabe, S. Collin, J.-F. Guillemoles, and Y. Okada, "Identification of surface and volume hot-carrier thermalization mechanisms in ultrathin GaAs layers," J. Appl. Phys. 128, 193102 (2020).
- ²⁷L. A. Pettersson, L. S. Roman, and O. Inganäs, "Modeling photocurrent action spectra of photovoltaic devices based on organic thin films," J. Appl. Phys. 86, 487–496 (1999)
- ²⁸P. Peumans, A. Yakimov, and S. R. Forrest, "Small molecular weight organic thin-film photodetectors and solar cells," J. Appl. Phys. 93, 3693–3723 (2003).
- ²⁹E. Grann, K.-T. Tsen, and D. Ferry, "Nonequilibrium phonon dynamics and electron distribution functions in InP and InAs," Phys. Rev. B 53, 9847 (1996).
- 30S. D. Sarma, J. K. Jain, and R. Jalabert, "Theory of hot-electron energy loss in polar semiconductors: Role of plasmon-phonon coupling," Phys. Rev. B 37, 6290 (1988).
- ³¹D. Ferry, "In search of a true hot carrier solar cell," Semicond. Sci. Technol. 34, 044001 (2019).
- ³²L. C. Hirst, M. K. Yakes, C. G. Bailey, J. G. Tischler, M. P. Lumb, M. Gonzalez, M. F. Führer, N. Ekins-Daukes, and R. J. Walters, "Enhanced hot-carrier effects in InAlAs/InGaAs quantum wells," IEEE J. Photovoltaics 4, 1526–1531 (2014).
- ⁵³D. Olego and M. Cardona, "Raman scattering by coupled LO-phonon-plasmon modes and forbidden TO-phonon Raman scattering in heavily doped p-type GaAs," Phys. Rev. B 24, 7217 (1981).
- ³⁴H. P. Piyathilaka, R. Sooriyagoda, H. Esmaielpour, V. R. Whiteside, T. D. Mishima, M. B. Santos, I. R. Sellers, and A. D. Bristow, "Hot-carrier dynamics in InAs/AlAsSb multi-quantum wells," arXiv:2103.03839 (2021).